Manufactured Solution for the 2D steady Favre–Averaged Navier–Stokes Equations with Spalart–Allmaras turbulence model

Kemelli C. Estacio-Hiroms*
Todd Oliver*

June 1, 2011

Contents

Abstract

The Method of Manufactured Solutions is a valuable approach for code verification, providing means to verify how accurately the numerical method solves the partial differential equations of interest. This document presents the source terms generated by the application of the Method of Manufactured Solutions on the 2D steady Favre–Averaged Navier–Stokes Equations with Spalart–Allmaras turbulence model using analytical manufactured solutions that reasonably resemble the inner portion (viscous sublayer and logarithmic layer) of a zero pressure gradient boundary layer.

*Center for Predictive Engineering and Computational Sciences (PECOS), Institute for Computational Engineering and Sciences, The University of Texas at Austin, Austin, TX 78712 ({kemelli,oliver}@ices.utexas.edu)

1 Mathematical Model

Turbulent flows occur at high Reynolds numbers, when the inertia of the fluid overwhelms the viscosity of the fluid, causing the laminar flow motions to become unstable. Under these conditions, the flow is characterized by rapid fluctuations in pressure and velocity which are inherently three dimensional and unsteady. Turbulent flow is composed of large eddies that migrate across the flow generating smaller eddies as they go. These smaller eddies in turn generates smaller eddies until they become small enough that their energy is dissipated due to the presence of molecular viscosity.

In practice, the effect of this sensitivity is to make the value of any flow quantity at any particular point in time and space uncertain. Thus, these quantities may be viewed as random variables with associated probability density functions, allowing the use of statistical techniques in the description and analysis of the flow. Or, in other words, the full influence of the turbulent fluctuations on the mean flow must be modeled.

For flows with significant density variations it is possible to capture the turbulent effects using the Favre averaged Navier-Stokes equations (FANS), together with baseline compressible Spalart–Allmaras (SA) turbulent model (Oliver, 2010; Spalart and Allmaras, 1994).

Mass conservation:

$$\frac{\partial \bar{\rho}}{\partial t} + \frac{\partial}{\partial x_i}(\bar{\rho}\tilde{u}_i) = 0, \tag{1}$$

Momentum conservation:

$$\frac{\partial}{\partial t}\left(\bar{\rho}\tilde{u}_i\right) + \frac{\partial}{\partial x_j}\left(\bar{\rho}\tilde{u}_j\tilde{u}_i\right) = -\frac{\partial \bar{p}}{\partial x_i} + \frac{\partial}{\partial x_j}\left(2(\bar{\mu}+\mu_t)\tilde{S}_{ji}\right), \tag{2}$$

Total energy conservation:

$$\frac{\partial}{\partial t}\left[\bar{\rho}\left(\tilde{e}+\frac{1}{2}\tilde{u}_i\tilde{u}_i\right)\right] + \frac{\partial}{\partial x_j}\left[\bar{\rho}\tilde{u}_j\left(\tilde{h}+\frac{1}{2}\tilde{u}_i\tilde{u}_i\right)\right] = \frac{\partial}{\partial x_j}\left(2(\bar{\mu}+\mu_t)\tilde{S}_{ji}\tilde{u}_i\right) + \frac{\partial}{\partial x_j}\left[\left(\frac{\bar{\mu}}{\mathrm{Pr}}+\frac{\mu_t}{\mathrm{Pr}_t}\right)\frac{\partial \tilde{h}}{\partial x_j}\right], \tag{3}$$

Baseline compressible Spalart–Allmaras equation:

$$\frac{\partial}{\partial t}(\bar{\rho}\nu_{\mathrm{sa}}) + \frac{\partial}{\partial x_j}(\bar{\rho}\tilde{u}_j\nu_{\mathrm{sa}}) = c_{b1}S_{\mathrm{sa}}\bar{\rho}\nu_{\mathrm{sa}} - c_{w1}f_w\bar{\rho}\left(\frac{\nu_{\mathrm{sa}}}{d}\right)^2 + \frac{1}{\sigma}\frac{\partial}{\partial x_k}\left[(\bar{\mu}+\bar{\rho}\nu_{\mathrm{sa}})\frac{\partial \nu_{\mathrm{sa}}}{\partial x_k}\right] + \frac{c_{b2}}{\sigma}\bar{\rho}\frac{\partial \nu_{\mathrm{sa}}}{\partial x_k}\frac{\partial \nu_{\mathrm{sa}}}{\partial x_k}, \tag{4}$$

where $[\tilde{\ }]$ denotes a Favre-averaging variable and $[\bar{\ }]$ denotes Reynolds averaging.

To close the equations, many additional relationships are necessary—e.g., a constitutive relation for the viscous stress, an equation of state, etc. In this work, the gas is considered calorically perfect and:

$$\begin{aligned}
&\bar{\mu} = \texttt{constant}, \quad \tilde{S}_{ij} = \tilde{s}_{ij} - \frac{1}{3}\tilde{s}_{kk}\delta_{ij}, \quad \tilde{s}_{ij} = \frac{1}{2}\left(\frac{\partial \tilde{u}_i}{\partial x_j} + \frac{\partial \tilde{u}_j}{\partial x_i}\right),\\
&\bar{p} = \bar{\rho}R\tilde{T}, \quad \tilde{e} = c_v\tilde{T}, \quad \tilde{h} = c_p\tilde{T} = \tilde{e} + \frac{\bar{p}}{\bar{\rho}}, \quad \mu_t = \bar{\rho}\nu_t = \bar{\rho}\nu_{\mathrm{sa}}f_{v1},\\
&S_{\mathrm{sa}} = \Omega + S_m, \quad \Omega = \sqrt{2\tilde{\Omega}_{ij}\tilde{\Omega}_{ij}}, \quad \tilde{\Omega}_{ij} = \frac{1}{2}\left(\frac{\partial \tilde{u}_i}{\partial x_j} - \frac{\partial \tilde{u}_j}{\partial x_i}\right),\\
&f_{v2} = 1 - \frac{\chi}{1+\chi f_{v1}}, \quad f_{v1} = \frac{\chi^3}{\chi^3 + c_{v1}^3}, \quad \chi = \frac{\nu_{\mathrm{sa}}}{\tilde{\nu}},\\
&f_w = g\left(\frac{1+c_{w3}^6}{g^6+c_{w3}^6}\right)^{1/6}, \quad g = r + c_{w2}\left(r^6 - r\right), \quad r = \frac{\nu_{\mathrm{sa}}}{S_{\mathrm{sa}}\kappa^2 d^2},
\end{aligned} \tag{5}$$

where d is the distance to the nearest no-slip wall. The constants c_v and c_p are fluid properties. The constants c_{b1}, c_{b2}, c_{v1}, σ, c_{w1}, c_{w2}, c_{w3}, and κ are the SA model calibration parameters.

Note that the S_{sa} function is modified to avoid bad behavior introduced by the f_{v2} function; S_m is defined as follows:

$$S_m = \begin{cases} S_{m,orig}, & S_{m,orig} \geq -c_{v2}\Omega \\ \dfrac{\Omega(c_{v2}^2\Omega + c_{v3}S_{m,orig})}{(c_{v3}-2.0c_{v2})\Omega - S_{m,orig}}, & \text{otherwise.} \end{cases}$$

with

$$S_{m,orig} = \frac{\nu_{\mathrm{sa}}}{\kappa^2 d^2}f_{v2}.$$

2 Manufactured Solutions

The Method of Manufactured Solutions (MMS) applied to Favre–Averaged Navier–Stokes equations with baseline compressible Spalart–Allmaras turbulence model consists in modifying Equations (1) – (4) by adding a source term to the right-hand side of each equation, so the modified set of equations conveniently has the analytical solution chosen *a priori*.

To exercise all of the terms in the equation, the solution must satisfy the no-slip wall boundary condition for at least some portion of the boundary. To avoid pathological behavior in the solution and required source terms, we strive to make the manufactured solution reasonably resemble the inner portion (viscous sublayer + logarithmic layer) of a zero pressure gradient boundary layer. To accomplish this goal, the manufactured solution is built using well-known correlations for turbulent boundary layers. For details, see Appendix A.

They are:

$$
\begin{aligned}
u &= \frac{u_\infty}{A}\sin\left(\frac{A}{u_\infty}u_{eq}\right),\\
v &= -\eta_v\frac{du_\tau}{dx}y,\\
T &= T_\infty\left[1 + r_T\frac{\gamma-1}{2}M_\infty^2\left(1-\left(\frac{u}{u_\infty}\right)^2\right)\right],\\
\rho &= \frac{p_0}{RT},\\
\nu_{\mathrm{sa}} &= \kappa u_\tau y - \alpha y^2.
\end{aligned}
\tag{6}
$$

The pressure is chosen to be a constant $p = p_0$. Values u_∞ and A are constants, η_v is a user-specified parameter. T_∞, M_∞, r_T, γ, κ and α are additional constant parameters.

The van Driest equivalent velocity u_{eq}, the friction velocity u_τ and the non-dimensionalized van Driest velocity profile u_{eq}^+ are given by:

$$
\begin{aligned}
u_{eq} &= u_\tau u_{eq}^+,\\
u_\tau &= u_\infty\sqrt{\frac{c_f}{2}},\\
u_{eq}^+ &= \frac{1}{\kappa}\log\left(1+\kappa y^+\right) + C_1\left[1 - e^{-y^+/\eta_1} - \frac{y^+}{\eta_1}e^{-y^+ b}\right]
\end{aligned}
\tag{7}
$$

with

$$
c_f = \frac{C_{cf}}{F_c}\left(\frac{Re_x}{F_c}\right)^{-1/7}, \quad Re_x = \frac{\rho_\infty u_\infty x}{\mu}, \quad \text{and} \quad y^+ = \frac{y u_\tau}{\nu_w},
$$

where η_1, b, $C_1 = -(1/\kappa)\log(\kappa) + C$, C, C_{cf}, F_c, ρ_∞, and ν_w are constants.

Additionally,

$$
\frac{du_{eq}^+}{dy^+} = \frac{1}{(1+\kappa y^+)} + C_1\left[\frac{1}{\eta_1}e^{-y^+/\eta_1} - \frac{1}{\eta_1}e^{-y^+ b} + b\frac{y^+}{\eta_1}e^{-y^+ b}\right]. \tag{8}
$$

Source terms for mass conservation (Q_ρ), momentum (Q_u, and Q_v), total energy (Q_E) and SA variable ($Q_{\nu_{\mathrm{sa}}}$) equations are obtained by symbolic manipulations of FANS equations with SA turbulence model above using Maple 13 (Maplesoft, 2010) and are presented in the following sections.

2.1 2D FANS Equations and SA Turbulence Model

MMS applied to the 2D steady FANS equations with SA turbulent model simply consists in modifying Equations (1) – (4) by adding a source term to the right-hand side of each equation:

$$
\begin{aligned}
&\frac{\partial(\bar{\rho})}{\partial t}+\nabla\cdot(\bar{\rho}\tilde{\boldsymbol{u}})=Q_{\bar{\rho}},\\
&\frac{\partial(\bar{\rho}\tilde{\boldsymbol{u}})}{\partial t}+\nabla\cdot(\bar{\rho}\tilde{\boldsymbol{u}}\tilde{\boldsymbol{u}})+\nabla\bar{p}-\nabla\cdot(2(\bar{\mu}+\mu_t)\tilde{\boldsymbol{S}})=Q_{\tilde{\boldsymbol{u}}},\\
&\frac{\partial(\bar{\rho}\tilde{E})}{\partial t}+\nabla\cdot(\bar{\rho}\tilde{\boldsymbol{u}}\tilde{H})-\nabla\cdot\bar{\boldsymbol{q}}-\nabla\cdot(2(\bar{\mu}+\mu_t)\tilde{\boldsymbol{S}}\cdot\tilde{\boldsymbol{u}})=Q_{\tilde{E}},\\
&\frac{\partial(\bar{\rho}\nu_{\mathrm{sa}})}{\partial t}+\nabla\cdot(\bar{\rho}\tilde{\boldsymbol{u}}\nu_{\mathrm{sa}})-c_{b1}S_{\mathrm{sa}}\bar{\rho}\nu_{\mathrm{sa}}+c_{w1}f_w\bar{\rho}\left(\frac{\nu_{\mathrm{sa}}}{d}\right)^2-\frac{1}{\sigma}\nabla\cdot((\bar{\mu}+\bar{\rho}\nu_{\mathrm{sa}})\nabla\nu_{\mathrm{sa}})-\frac{c_{b2}\bar{\rho}}{\sigma}\nabla\nu_{\mathrm{sa}}\cdot\nabla\nu_{\mathrm{sa}}=Q_{\nu_{\mathrm{sa}}},
\end{aligned}
\tag{9}
$$

so the modified set of Equations (9) has Equation (6) as analytical solution.

Recall that the averaged kinematic viscosity, total energy per unit mass and the total enthalpy per unit mass are given, respectively, by:

$$
\tilde{\nu}=\frac{\bar{\mu}}{\bar{\rho}},\qquad \tilde{E}=\tilde{e}+\frac{\tilde{\boldsymbol{u}}\cdot\tilde{\boldsymbol{u}}}{2},\quad \tilde{H}=\tilde{h}+\frac{\tilde{\boldsymbol{u}}\cdot\tilde{\boldsymbol{u}}}{2},
\tag{10}
$$

with $\tilde{e}$ and $\tilde{h}$ defined in Equation (5). The averaged absolute viscosity $\bar{\mu}$ is assumed to be constant.

The laminar mean heat-flux vector $\bar{\boldsymbol{q}}=(\bar{q}_x,\bar{q}_y)$ is given by:

$$
\bar{q}_x=\left(\frac{\bar{\mu}}{\mathrm{Pr}}+\frac{\mu_t}{\mathrm{Pr}_t}\right)\frac{\partial\tilde{h}}{\partial x}\quad\text{and}\quad \bar{q}_y=\left(\frac{\bar{\mu}}{\mathrm{Pr}}+\frac{\mu_t}{\mathrm{Pr}_t}\right)\frac{\partial\tilde{h}}{\partial y},
\tag{11}
$$

where the Prandtl number, Pr, and the turbulent Prandtl number, Pr_t, are also assumed to be constant.

Additionally, Ω and $\tilde{\boldsymbol{S}}$ in expression (5) are:

$$
\Omega=\sqrt{\left(\frac{\partial\tilde{u}}{\partial y}-\frac{\partial\tilde{v}}{\partial x}\right)^2}\quad\text{and}\quad \tilde{\boldsymbol{S}}=\begin{bmatrix}\tilde{S}_{xx} & \tilde{S}_{xy}\\ \tilde{S}_{yx} & \tilde{S}_{yy}\end{bmatrix},
$$

with

$$
\tilde{S}_{xx}=\frac{\partial\tilde{u}}{\partial x}-\frac{1}{3}\nabla\cdot\tilde{\boldsymbol{u}},\quad \tilde{S}_{yy}=\frac{\partial\tilde{v}}{\partial y}-\frac{1}{3}\nabla\cdot\tilde{\boldsymbol{u}},\quad \tilde{S}_{xy}=\tilde{S}_{yx}=\left(\frac{\partial\tilde{u}}{\partial y}+\frac{\partial\tilde{v}}{\partial x}\right).
$$

Source terms $Q_{\bar{\rho}}$, $Q_{\tilde{u}}$, $Q_{\tilde{v}}$, $Q_{\tilde{E}}$ and $Q_{\nu_{\mathrm{sa}}}$ are presented in the subsequent sessions with the use of the auxiliary variables:

$$
\begin{aligned}
\mathtt{U}&=\frac{u_\infty}{A}\sin\left(\frac{A}{u_\infty}u_{eq}\right),\\
\mathtt{V}&=\frac{1}{14}\frac{\eta_v u_\tau y}{x},\\
\mathtt{T}&=T_\infty\left[1+r_T\frac{\gamma-1}{2}M_\infty^2\left(1-\left(\frac{u}{u_\infty}\right)^2\right)\right],\\
\mathtt{Rho}&=\frac{p_0}{RT},\\
\mathtt{Nu_{sa}}&=\kappa u_\tau y-\alpha y^2,
\end{aligned}
\tag{12}
$$

which simply are the manufactured solutions, and the derivatives:

$$
\begin{aligned}
\frac{\partial^2 u_{eq}}{\partial x^2} &= -\frac{1}{196}\frac{u_\tau (y^+)^2}{\eta_1 x^2}\,\frac{du^+_{eq}}{dy^+} - \frac{1}{196}\frac{C_1 u_\tau (y^+)^2 (b^2\eta_1 y^+ - by^+ + 1 - 2b\eta_1)\exp(-by^+)}{\eta_1^2 x^2} + \\
&\quad + \frac{1}{196}\frac{u_\tau (y^+)^2(\kappa y^+ + \kappa\eta_1 + 1)}{\eta_1(\kappa y^+ + 1)^2 x^2} + \frac{17}{196}\frac{y^+ u_\tau}{x^2}\,\frac{du^+_{eq}}{dy^+} + \frac{15}{196}\frac{u_\tau u^+_{eq}}{x^2}, \\
\frac{\partial^2 u_{eq}}{\partial y^2} &= -\frac{u_\tau (y^+)^2}{\eta_1 y^2}\,\frac{du^+_{eq}}{dy^+} + u_\tau (y^+)^2\left(-\frac{C_1(b^2\eta_1 y^+ - by^+ + 1 - 2b\eta_1)\exp(-by^+)}{\eta_1^2 y^2} + \frac{\kappa y^+ - \kappa\eta_1 + 1}{\eta_1(\kappa y^+ + 1)^2 y^2}\right), \\
\frac{\partial^2 u}{\partial x^2} &= -\frac{1}{196}\frac{A^2 u_\tau^2\,\mathtt{U}}{u_\infty^2 x^2}\left[u^+_{eq} + y^+\,\frac{du^+_{eq}}{dy^+}\right]^2 + \cos\left(\frac{A u_{eq}}{u_\infty}\right)\frac{\partial^2 u_{eq}}{\partial x^2}, \\
\frac{\partial^2 u}{\partial y^2} &= -\frac{A^2 u_\tau^2 (y^+)^2\,\mathtt{U}}{u_\infty^2 y^2}\left(\frac{du^+_{eq}}{dy^+}\right)^2 + \cos\left(\frac{A u_{eq}}{u_\infty}\right)\frac{\partial^2 u_{eq}}{\partial y^2}, \\
\frac{\partial^2 u}{\partial x y} &= \frac{1}{14}\frac{A^2 u_\tau^2 y^+\,\mathtt{U}}{u_\infty^2 x y}\,\frac{du^+_{eq}}{dy^+}\left[u^+_{eq} + y^+\,\frac{du^+_{eq}}{dy^+}\right], \\
\frac{\partial^2 v}{\partial x^2} &= \frac{435}{196}\frac{\mathtt{V}}{x^2}, \\
\frac{\partial^2 v}{\partial y^2} &= 0, \\
\frac{\partial^2 v}{\partial x y} &= -\frac{15}{14}\frac{\mathtt{V}}{xy}, \\
\frac{\partial^2 T}{\partial x^2} &= \frac{1}{196}\frac{r_T\,(\gamma-1)\,M_\infty^2\,T_\infty u_\tau^2}{u_\infty^2\,x^2}\left[\cos\left(\frac{A u_{eq}}{u_\infty}\right)^2 - \sin\left(\frac{A u_{eq}}{u_\infty}\right)^2\right]\left[u^+_{eq} + y^+\,\frac{du^+_{eq}}{dy^+}\right]^2 + \\
&\quad + \frac{r_T\,(\gamma-1)\,M_\infty^2\,T_\infty}{A\,u_\infty}\sin\left(\frac{A u_{eq}}{u_\infty}\right)\cos\left(\frac{A u_{eq}}{u_\infty}\right)\frac{\partial^2 u_{eq}}{\partial x^2}, \\
\frac{\partial^2 T}{\partial y^2} &= \frac{r_T\,(\gamma-1)\,M_\infty^2\,T_\infty u_\tau^2 (y^+)^2}{u_\infty^2\,y^2}\left[\cos\left(\frac{A u_{eq}}{u_\infty}\right)^2 - \sin\left(\frac{A u_{eq}}{u_\infty}\right)^2\right]\left(\frac{du^+_{eq}}{dy^+}\right)^2 + \\
&\quad + \frac{r_T\,(\gamma-1)\,M_\infty^2\,T_\infty}{A\,u_\infty}\sin\left(\frac{A u_{eq}}{u_\infty}\right)\cos\left(\frac{A u_{eq}}{u_\infty}\right)\frac{\partial^2 u_{eq}}{\partial y^2}, \\
\frac{du^+_{eq}}{dy^+} &= \frac{1}{1+\kappa y^+} + C_1\left(\frac{\exp(\frac{-y^+}{\eta_1})}{\eta_1} - \frac{\exp(-b\,y^+)}{\eta_1} + \frac{b\,y^+\exp(-b\,y^+)}{\eta_1}\right).
\end{aligned}
\tag{13}
$$

2.1.1 2D FANS Mass Conservation

The 2D Favre-averaged mass conservation equation written as an operator is:

$$
\mathcal{L} = \frac{\partial(\bar\rho)}{\partial t} + \frac{\partial(\bar\rho\tilde u)}{\partial x} + \frac{\partial(\bar\rho\tilde v)}{\partial y}.
$$

Analytically differentiating Equation (6) for $\bar\rho$, $\tilde u$ and $\tilde v$ using operator $\mathcal{L}$ defined above gives the source term $Q_{\bar\rho}$:

$$
\begin{aligned}
Q_{\bar\rho} &= \frac{1}{14}\frac{r_T\,(\gamma-1)\,M_\infty^2\,T_\infty\,u_\tau\,\mathtt{Rho}\,\mathtt{U}^2}{u_\infty^2\,x\,\mathtt{T}}\cos\left(\frac{A u_{eq}}{u_\infty}\right)\left[y^+\,\frac{du^+_{eq}}{dy^+} + u^+_{eq}\right] + \\
&\quad - \frac{r_T\,(\gamma-1)\,M_\infty^2\,T_\infty\,y^+\,u_\tau\,\mathtt{Rho}\,\mathtt{U}\,\mathtt{V}}{u_\infty^2\,y\,\mathtt{T}}\,\frac{du^+_{eq}}{dy^+}\cos\left(\frac{A u_{eq}}{u_\infty}\right) + \\
&\quad - \frac{1}{14}\frac{u_\tau\,\mathtt{Rho}}{x}\cos\left(\frac{A u_{eq}}{u_\infty}\right)\left[y^+\,\frac{du^+_{eq}}{dy^+} + u^+_{eq}\right] + \\
&\quad + \frac{\mathtt{Rho}\,\mathtt{V}}{y},
\end{aligned}
\tag{14}
$$

where `Rho`, `U`, `V` and `T` are given in Equation (12), and $\frac{du^+_{eq}}{dy^+}$ is defined in Equation (8).

2.1.2 2D FANS Momentum Conservation

For the generation of the analytical source term $Q_{\tilde{u}}$ for the Favre-averaged x-momentum equation, the first component of Equation (2) is written as an operator $\mathcal{L}$:

$$\mathcal{L} = \frac{\partial(\bar{\rho}\tilde{u})}{\partial t} + \frac{\partial(\bar{\rho}\tilde{u}^2)}{\partial x} + \frac{\partial(\bar{\rho}\tilde{u}\tilde{v})}{\partial y} + \frac{\partial(\bar{p})}{\partial x} - \frac{\partial(2(\bar{\mu}+\mu_t)\tilde{S}_{xx})}{\partial x} - \frac{\partial(2(\bar{\mu}+\mu_t)\tilde{S}_{xy})}{\partial y},$$

which, when operated in Equation (6), provides source term $Q_{\tilde{u}}$:

$$\begin{aligned}
Q_{\tilde{u}} = & \frac{1}{14}\frac{r_T\,(\gamma-1)\,M_\infty^2\,T_\infty\,u_\tau\,\texttt{Rho}\,\texttt{U}^3}{u_\infty^2\,x\,\texttt{T}}\cos\left(\frac{Au_{eq}}{u_\infty}\right)\left[y^+\,\frac{du_{eq}^+}{dy^+}+u_{eq}^+\right]+\\
& +\frac{1}{147}\frac{\mu_t\,r_T\,(\gamma-1)\,M_\infty^2\,T_\infty\,u_\tau^2\,\texttt{U}}{u_\infty^2\,x^2\,\texttt{T}}\cos\left(\frac{Au_{eq}}{u_\infty}\right)^2\left[y^+\,\frac{du_{eq}^+}{dy^+}+u_{eq}^+\right]^2+\\
& -\frac{r_T\,(\gamma-1)\,M_\infty^2\,T_\infty\,y^+\,u_\tau\,\texttt{Rho}\,\texttt{U}^2\,\texttt{V}}{u_\infty^2\,y\,\texttt{T}}\,\frac{du_{eq}^+}{dy^+}\cos\left(\frac{Au_{eq}}{u_\infty}\right)+\\
& +\frac{\mu_t\,r_T\,(\gamma-1)\,M_\infty^2\,T_\infty\,(y^+)^2\,u_\tau^2\,\texttt{U}}{u_\infty^2\,y^2\,\texttt{T}}\left(\frac{du_{eq}^+}{dy^+}\right)^2\cos\left(\frac{Au_{eq}}{u_\infty}\right)^2+\\
& -\frac{1}{42}\frac{\mu_t\,r_T\,(\gamma-1)\,M_\infty^2\,T_\infty\,u_\tau\,\texttt{U}\,\texttt{V}}{u_\infty^2\,xy\,\texttt{T}}\cos\left(\frac{Au_{eq}}{u_\infty}\right)\left[43y^+\,\frac{du_{eq}^+}{dy^+}-2u_{eq}^+\right]+\\
& +\frac{y^+u_\tau\,\texttt{Rho}\,\texttt{V}}{y}\,\frac{du_{eq}^+}{dy^+}\cos\left(\frac{Au_{eq}}{u_\infty}\right)+\\
& -\frac{1}{7}\frac{u_\tau\,\texttt{Rho}\,\texttt{U}}{x}\cos\left(\frac{Au_{eq}}{u_\infty}\right)\left[y^+\,\frac{du_{eq}^+}{dy^+}+u_{eq}^+\right]+\\
& +\frac{\texttt{Rho}\,\texttt{U}\,\texttt{V}}{y}+\\
& -2(\mu+\mu_t)\left[\frac{2}{3}\frac{\partial^2 u}{\partial x^2}+\frac{1}{6}\frac{\partial^2 v}{\partial xy}+\frac{1}{2}\frac{\partial^2 u}{\partial y^2}\right],
\end{aligned} \tag{15}$$

where `Rho`, `U`, `V` and `T` are given in Equation (12). The derivatives are given in Equations (8) and (13), and

$$\mu_t = f_{v1}\,\texttt{Rho}\,\texttt{Nu}_{\texttt{sa}},\quad f_{v1} = \frac{\chi^3}{\chi^3+c_{v1}^3}\quad\text{and}\quad \chi = \frac{\texttt{Nu}_{\texttt{sa}}}{\tilde{\nu}} = \frac{\texttt{Rho}\,\texttt{Nu}_{\texttt{sa}}}{\bar{\mu}}, \tag{16}$$

which is consistent with the definition in Equation (5).

Analogously, for the generation of the analytical source term $Q_{\tilde{v}}$ for the Favre-averaged y-momentum equation, the second component of Equation (2) is written as an operator $\mathcal{L}$:

$$\mathcal{L} = \frac{\partial(\bar{\rho}\tilde{v})}{\partial t} + \frac{\partial(\bar{\rho}\tilde{u}\tilde{v})}{\partial x} + \frac{\partial(\bar{\rho}\tilde{v}^2)}{\partial y} + \frac{\partial(\bar{p})}{\partial y} - \frac{\partial(2(\bar{\mu}+\mu_t)\tilde{S}_{yx})}{\partial x} - \frac{\partial(2(\bar{\mu}+\mu_t)\tilde{S}_{yy})}{\partial y},$$

and then applied to Equation (6). It yields:

$$
\begin{aligned}
Q_{\tilde{v}} = & \frac{1}{14}\frac{r_T\,(\gamma-1)\,M_\infty^2\,T_\infty\,u_\tau\,\mathtt{Rho}\,\mathtt{U}^2\,\mathtt{V}}{u_\infty^2\,x\,\mathtt{T}}\cos\left(\frac{Au_{eq}}{u_\infty}\right)\left[y^+\frac{du_{eq}^+}{dy^+}+u_{eq}^+\right]+\\
&+\frac{15}{196}\frac{\mu_t\,r_T\,(\gamma-1)\,M_\infty^2\,T_\infty\,u_\tau\,\mathtt{U}\,\mathtt{V}}{u_\infty^2\,x^2\,\mathtt{T}}\cos\left(\frac{Au_{eq}}{u_\infty}\right)\left[y^+\frac{du_{eq}^+}{dy^+}+u_{eq}^+\right]+\\
&-\frac{1}{42}\frac{\mu_t\,r_T\,(\gamma-1)\,M_\infty^2\,T_\infty\,y^+\,u_\tau^2\,\mathtt{U}}{u_\infty^2\,xy\,\mathtt{T}}\frac{du_{eq}^+}{dy^+}\cos\left(\frac{Au_{eq}}{u_\infty}\right)^2\left[y^+\frac{du_{eq}^+}{dy^+}+u_{eq}^+\right]+\\
&-\frac{r_T\,(\gamma-1)\,M_\infty^2\,T_\infty\,y^+\,u_\tau\,\mathtt{Rho}\,\mathtt{U}\,\mathtt{V}^2}{u_\infty^2\,y\,\mathtt{T}}\frac{du_{eq}^+}{dy^+}\cos\left(\frac{Au_{eq}}{u_\infty}\right)+\\
&+\frac{4}{3}\frac{\mu_t\,r_T\,(\gamma-1)\,M_\infty^2\,T_\infty\,y^+\,u_\tau\,\mathtt{U}\,\mathtt{V}}{u_\infty^2\,y^2\,\mathtt{T}}\frac{du_{eq}^+}{dy^+}\cos\left(\frac{Au_{eq}}{u_\infty}\right)+\\
&-\frac{1}{14}\frac{u_\tau\,\mathtt{Rho}\,\mathtt{V}}{x}\cos\left(\frac{Au_{eq}}{u_\infty}\right)\left[y^+\frac{du_{eq}^+}{dy^+}+u_{eq}^+\right]+\\
&-\frac{15}{14}\frac{\mathtt{Rho}\,\mathtt{U}\,\mathtt{V}}{x}\quad+\quad\frac{2\,\mathtt{Rho}\,\mathtt{V}^2}{y}+\\
&-2(\mu+\mu_t)\left[\frac{1}{6}\frac{\partial^2 u}{\partial xy}+\frac{1}{2}\frac{\partial^2 v}{\partial x^2}+\frac{2}{3}\frac{\partial^2 v}{\partial y^2}\right],
\end{aligned}
\tag{17}
$$

where Rho, U, V and T are given in Equation (12), the derivatives are given in Equations (8) and (13), and μ_t is given in Equation (16).

2.1.3 2D FANS Total Energy Conservation

The operator for the 2D Favre-averaged total energy is:

$$
\begin{aligned}
\mathcal{L} = & \frac{\partial(\bar\rho\tilde E)}{\partial t}+\frac{\partial(\bar\rho\tilde u\tilde E)}{\partial x}+\frac{\partial(\bar\rho\tilde v\tilde E)}{\partial y}+\frac{\partial(\bar p\tilde u)}{\partial x}+\frac{\partial(\bar p\tilde v)}{\partial y}-\frac{\partial(\bar q_x)}{\partial x}-\frac{\partial(\bar q_y)}{\partial y}+\\
&-\frac{\partial(2(\bar\mu+\mu_t)\tilde u\tilde S_{xx})}{\partial x}-\frac{\partial(2(\bar\mu+\mu_t)\tilde v\tilde S_{xy})}{\partial x}-\frac{\partial(2(\bar\mu+\mu_t)\tilde u\tilde S_{yx})}{\partial y}-\frac{\partial(2(\bar\mu+\mu_t)\tilde v\tilde S_{yy})}{\partial y}.
\end{aligned}
$$

Source term $Q_{\tilde E}$ is obtained by operating $\mathcal{L}$ on Equation (6) together with the use of the auxiliary relations for energy given in Equations (5), (10) and (11). It yields:

$$
\begin{aligned}
Q_{\tilde E} = & +\frac{1}{196}\frac{\mu_t\,c_p\,r_T^2\,(\gamma-1)^2\,M_\infty^4\,T_\infty^2\,u_\tau^2\,\mathtt{U}^2}{u_\infty^4\,x^2 Pr_t\,\mathtt{T}}\cos\left(\frac{Au_{eq}}{u_\infty}\right)^2\left[y^+\frac{du_{eq}^+}{dy^+}+u_{eq}^+\right]^2+\\
&+\frac{1}{147}\frac{\mu_t\,r_T\,(\gamma-1)\,M_\infty^2\,T_\infty\,u_\tau^2\,\mathtt{U}^2}{u_\infty^2\,x^2\,\mathtt{T}}\cos\left(\frac{Au_{eq}}{u_\infty}\right)^2\left[y^+\frac{du_{eq}^+}{dy^+}+u_{eq}^+\right]^2+\\
&+\frac{15}{196}\frac{\mu_t\,r_T\,(\gamma-1)\,M_\infty^2\,T_\infty\,u_\tau\,\mathtt{U}\,\mathtt{V}^2}{u_\infty^2\,x^2\,\mathtt{T}}\cos\left(\frac{Au_{eq}}{u_\infty}\right)\left[y^+\frac{du_{eq}^+}{dy^+}+u_{eq}^+\right]+\\
&-\frac{1}{196}\frac{y\,f_{v1}\,\kappa\,c_p\,r_T\,(\gamma-1)\,M_\infty^2\,T_\infty\,u_\tau^2\,\mathtt{Rho}\,\mathtt{U}}{u_\infty^2\,x^2 Pr_t}\cos\left(\frac{Au_{eq}}{u_\infty}\right)\left[y^+\frac{du_{eq}^+}{dy^+}+u_{eq}^+\right]+\\
&+\frac{1}{28}\frac{r_T\,(\gamma-1)\,M_\infty^2\,T_\infty\,u_\tau\,\mathtt{Rho}\,\mathtt{U}^2(\mathtt{U}^2+\mathtt{V}^2)}{u_\infty^2\,x\,\mathtt{T}}\cos\left(\frac{Au_{eq}}{u_\infty}\right)\left[y^+\frac{du_{eq}^+}{dy^+}+u_{eq}^+\right]+\\
&+\frac{\mu_t\,c_p\,r_T^2\,(\gamma-1)^2\,M_\infty^4\,T_\infty^2\,(y^+)^2\,u_\tau^2\,\mathtt{U}^2}{u_\infty^4\,y^2 Pr_t\,\mathtt{T}}\left(\frac{du_{eq}^+}{dy^+}\right)^2\cos\left(\frac{Au_{eq}}{u_\infty}\right)^2+\\
&+\cdots
\end{aligned}
$$

$$
\begin{aligned}
&+\cdots\\
&+\frac{\mu_t\, r_T\,(\gamma-1)\,M_\infty^2\,T_\infty\,(y^+)^2\,u_\tau^2\;\mathtt{U}^2}{u_\infty^2\,y^2\,\mathtt{T}}\left(\frac{du_{eq}^+}{dy^+}\right)^2\cos\left(\frac{Au_{eq}}{u_\infty}\right)^2+\\
&+\frac{4}{3}\frac{\mu_t\, r_T\,(\gamma-1)\,M_\infty^2\,T_\infty\,y^+\,u_\tau\;\mathtt{U}\,\mathtt{V}^2}{u_\infty^2\,y^2\,\mathtt{T}}\frac{du_{eq}^+}{dy^+}\cos\left(\frac{Au_{eq}}{u_\infty}\right)+\\
&-\frac{1}{2}\frac{r_T\,(\gamma-1)\,M_\infty^2\,T_\infty\,y^+\,u_\tau\;\mathtt{Rho}\,\mathtt{U}\,\mathtt{V}(\mathtt{U}^2+\mathtt{V}^2)}{u_\infty^2\,y\,\mathtt{T}}\frac{du_{eq}^+}{dy^+}\cos\left(\frac{Au_{eq}}{u_\infty}\right)+\\
&+\frac{f_{v1}\,c_p\,r_T\,(2\alpha y-\kappa u_\tau)\,(\gamma-1)\,M_\infty^2\,T_\infty\,y^+\,u_\tau\;\mathtt{Rho}\,\mathtt{U}}{u_\infty^2\,yPr_t}\frac{du_{eq}^+}{dy^+}\cos\left(\frac{Au_{eq}}{u_\infty}\right)+\\
&-\frac{1}{42}\frac{\mu_t\, r_T\,(\gamma-1)\,M_\infty^2\,T_\infty\,u_\tau\;\mathtt{U}^2\,\mathtt{V}}{u_\infty^2\,xy\,\mathtt{T}}\cos\left(\frac{Au_{eq}}{u_\infty}\right)\left[43y^+\frac{du_{eq}^+}{dy^+}-2u_{eq}^+\right]+\\
&-\frac{1}{42}\frac{\mu_t\, r_T\,(\gamma-1)\,M_\infty^2\,T_\infty\,y^+\,u_\tau{}^2\;\mathtt{U}\,\mathtt{V}}{u_\infty^2\,xy\,\mathtt{T}}\frac{du_{eq}^+}{dy^+}\cos\left(\frac{Au_{eq}}{u_\infty}\right)^2\left[y^+\frac{du_{eq}^+}{dy^+}+u_{eq}^+\right]+\\
&-\frac{1}{147}\frac{\kappa\,f_{v1}\,y\,u_\tau^2\;\mathtt{Rho}\,\mathtt{U}}{x^2}\cos\left(\frac{Au_{eq}}{u_\infty}\right)\left[y^+\frac{du_{eq}^+}{dy^+}+u_{eq}^+\right]+\\
&-\frac{15}{196}\frac{\kappa\,f_{v1}\,y\,u_\tau\;\mathtt{Rho}\,\mathtt{V}^2}{x^2}+\\
&+\frac{1}{42}\frac{\kappa\,f_{v1}\,u_\tau^2\;\mathtt{Rho}\,\mathtt{V}}{x}\cos\left(\frac{Au_{eq}}{u_\infty}\right)\left[y^+\frac{du_{eq}^+}{dy^+}-2u_{eq}^+\right]+\\
&-\frac{1}{28}\frac{(3\,\mathtt{U}^2+\mathtt{V}^2+2c_p\,\mathtt{T})u_\tau\,\mathtt{Rho}}{x}\cos\left(\frac{Au_{eq}}{u_\infty}\right)\left[y^+\frac{du_{eq}^+}{dy^+}+u_{eq}^+\right]+\\
&+\frac{2}{21}\frac{\alpha\,f_{v1}\,y\,u_\tau\;\mathtt{Rho}\,\mathtt{V}}{x}\cos\left(\frac{Au_{eq}}{u_\infty}\right)\left[y^+\frac{du_{eq}^+}{dy^+}+u_{eq}^+\right]+\\
&-\frac{1}{42}\frac{f_{v1}(90\alpha y-43\kappa\,u_\tau)\,\mathtt{Rho}\,\mathtt{U}\,\mathtt{V}}{x}\\
&-\frac{15}{14}\frac{\mathtt{Rho}\,\mathtt{U}\,\mathtt{V}^2}{x}+\\
&+\frac{f_{v1}(\,2\alpha\,y-\kappa\,u_\tau)y^+\,u_\tau\;\mathtt{Rho}\,\mathtt{U}}{y}\frac{du_{eq}^+}{dy^+}\cos\left(\frac{Au_{eq}}{u_\infty}\right)+\\
&+\frac{y^+u_\tau\,\mathtt{Rho}\,\mathtt{U}\,\mathtt{V}}{y}\frac{du_{eq}^+}{dy^+}\cos\left(\frac{Au_{eq}}{u_\infty}\right)+\\
&+\frac{1}{2}\frac{(\,\mathtt{U}^2+3\,\mathtt{V}^2+2c_p\,\mathtt{T})\,\mathtt{Rho}\,\mathtt{V}}{y}+\\
&+\frac{4}{3}\frac{f_{v1}(\,2\alpha\,y-\kappa\,u_\tau)\,\mathtt{Rho}\,\mathtt{V}^2}{y}+\\
&-2(\mu+\mu_t)\left\{\frac{1}{2}\frac{(y^+)^2u_\tau^2}{y^2}\left(\frac{du_{eq}^+}{dy^+}\right)^2\cos\left(\frac{Au_{eq}}{u_\infty}\right)^2+\right.\\
&\qquad+\frac{1}{294}\frac{u_\tau^2}{x^2}\cos\left(\frac{Au_{eq}}{u_\infty}\right)^2\left[y^+\frac{du_{eq}^+}{dy^+}+u_{eq}^+\right]^2-\frac{1}{42}\frac{u_\tau\,\mathtt{V}}{xy}\cos\left(\frac{Au_{eq}}{u_\infty}\right)\left[43y^+\frac{du_{eq}^+}{dy^+}-2u_{eq}^+\right]+\\
&\qquad\left.+\mathtt{U}\left[\frac{2}{3}\frac{\partial^2u}{\partial x^2}+\frac{1}{6}\frac{\partial^2v}{\partial xy}+\frac{1}{2}\frac{\partial^2u}{\partial y^2}\right]+\mathtt{V}\left[\frac{1}{6}\frac{\partial^2u}{\partial xy}+\frac{1}{2}\frac{\partial^2v}{\partial x^2}+\frac{2}{3}\frac{\partial^2v}{\partial y^2}\right]+\frac{225}{392}\frac{\mathtt{V}^2}{x^2}+\frac{2}{3}\frac{\mathtt{V}^2}{y^2}\right\}+\\
&-c_p\left(\frac{\mu}{Pr}+\frac{\mu_t}{Pr_t}\right)\left[\frac{\partial^2T}{\partial x^2}+\frac{\partial^2T}{\partial y^2}\right]
\end{aligned}
\tag{18}
$$

where Rho, U, V and T are given in Equation (12), the derivatives are given in Equations (8) and (13), and μ_t and f_{v1} are given in Equation (16).

2.1.4 2D SA Transport Equation

The operator for the viscosity-like baseline compressible Spalart–Allmaras equation is:

$$\mathcal{L} = \frac{\partial(\bar\rho\nu_{\rm sa})}{\partial t} + \frac{\partial(\bar\rho\tilde u\nu_{\rm sa})}{\partial x} + \frac{\partial(\bar\rho\tilde v\nu_{\rm sa})}{\partial y} - c_{b1}S_{\rm sa}\bar\rho\nu_{\rm sa} + c_{w1}f_w\bar\rho\left(\frac{\nu_{\rm sa}}{d}\right)^2 + \\ -\frac{1}{\sigma}\left[\frac{\partial}{\partial x}\left((\bar\mu+\bar\rho\nu_{\rm sa})\frac{\partial\nu_{\rm sa}}{\partial x}\right) + \frac{\partial}{\partial y}\left((\bar\mu+\bar\rho\nu_{\rm sa})\frac{\partial\nu_{\rm sa}}{\partial y}\right)\right] - \frac{c_{b2}\bar\rho}{\sigma}\left[\left(\frac{\partial\nu_{\rm sa}}{\partial x}\right)^2 + \left(\frac{\partial\nu_{\rm sa}}{\partial y}\right)^2\right].$$

with $S_{\rm sa} = \Omega + S_m$ and

$$S_m = \begin{cases} S_{m,orig}, & S_{m,orig} \geq -c_{v2}\Omega \\ \dfrac{\Omega(c_{v2}^2\Omega + c_{v3}S_{m,orig})}{(c_{v3}-2.0c_{v2})\Omega - S_{m,orig}}, & \text{otherwise.}\end{cases}$$

Source term $Q_{\nu_{\rm sa}}$ is obtained by operating $\mathcal{L}$ on Equation (6) together with the use of the auxiliary relations given in Equation (5). It yields:

$$\begin{aligned} Q_{\nu_{\rm sa}} = {} & \frac{1}{196}\frac{y\,\kappa\,r_T\,(\gamma-1)\,M_\infty^2\,T_\infty\,u_\tau^2\,\texttt{Nu}_{\texttt{sa}}\,\texttt{Rho}\,\texttt{U}}{\sigma\,u_\infty^2\,x^2\,\texttt{T}}\cos\left(\frac{Au_{eq}}{u_\infty}\right)\left[y^+\frac{du_{eq}^+}{dy^+}+u_{eq}^+\right] + \\ & -\frac{r_T\,(2\alpha y-\kappa u_\tau)\,(\gamma-1)\,M_\infty^2\,T_\infty\,y^+u_\tau\,\texttt{Nu}_{\texttt{sa}}\,\texttt{Rho}\,\texttt{U}}{\sigma\,u_\infty^2\,y\,\texttt{T}}\frac{du_{eq}^+}{dy^+}\cos\left(\frac{Au_{eq}}{u_\infty}\right) + \\ & +\frac{1}{14}\frac{r_T\,(\gamma-1)\,M_\infty^2\,T_\infty\,u_\tau\,\texttt{Nu}_{\texttt{sa}}\,\texttt{Rho}\,\texttt{U}^2}{u_\infty^2\,x\,\texttt{T}}\cos\left(\frac{Au_{eq}}{u_\infty}\right)\left[y^+\frac{du_{eq}^+}{dy^+}+u_{eq}^+\right] + \\ & -\frac{r_T\,(\gamma-1)\,M_\infty^2\,T_\infty\,y^+\,u_\tau\,\texttt{Nu}_{\texttt{sa}}\,\texttt{Rho}\,\texttt{U}\,\texttt{V}}{u_\infty^2\,y\,\texttt{T}}\frac{du_{eq}^+}{dy^+}\cos\left(\frac{Au_{eq}}{u_\infty}\right) + \\ & -\frac{1}{14}\frac{\kappa y u_\tau\,\texttt{Rho}\,\texttt{U}}{x} + \\ & -\frac{1}{14}\frac{u_\tau\,\texttt{Nu}_{\texttt{sa}}\,\texttt{Rho}}{x}\cos\left(\frac{Au_{eq}}{u_\infty}\right)\left[y^+\frac{du_{eq}^+}{dy^+}+u_{eq}^+\right] + \\ & +\frac{1}{196}\frac{(\texttt{Nu}_{\texttt{sa}}\,\texttt{Rho}+\mu)(392\alpha x^2-15\kappa y u_\tau)}{\sigma x^2} + \\ & -\frac{1}{196}\frac{\kappa^2(1+c_{b2})y^2u_\tau^2\,\texttt{Rho}}{\sigma x^2} + \\ & +\frac{\texttt{Nu}_{\texttt{sa}}\,\texttt{Rho}\,\texttt{V}}{y} + \\ & -\frac{(2\alpha y-\kappa u_\tau)^2(1+c_{b2})\,\texttt{Rho}}{\sigma} \quad + \quad \frac{c_{w1}f_w\,\texttt{Rho}\,\texttt{Nu}_{\texttt{sa}}^{\,2}}{d^2} + \\ & -(2\alpha y-\kappa u_\tau)\,\texttt{Rho}\,\texttt{V} \quad - \quad c_{b1}S_{\rm sa}\,\texttt{Nu}_{\texttt{sa}}\,\texttt{Rho}, \end{aligned} \tag{19}$$

where Rho, U, V, T and $\texttt{Nu}_{\texttt{sa}}$ are defined in (12), f_{v1} is given in Equation (16), and

$$\begin{aligned} \Omega &= \frac{1}{196}\sqrt{\frac{u_\tau^2}{x^4y^2}\left(196x^2(y^+)\,\frac{du_{eq}^+}{dy^+}\,\cos\left(\frac{Au_{eq}}{u_\infty}\right)+15\eta_v y^2\right)^2} \\ f_{v2} &= 1-\frac{\chi}{1+\chi f_{v1}}, \qquad f_w = g\left(\frac{1+c_{w3}^6}{g^6+c_{w3}^6}\right)^{1/6}, \\ g &= r + c_{w2}\left(r^6-r\right), \qquad r = \frac{\texttt{Nu}_{\texttt{sa}}}{S_{\rm sa}\kappa^2d^2}, \\ S_{\rm sa} &= \Omega + S_m, \quad S_{m,orig} = \frac{\texttt{Nu}_{\texttt{sa}}}{\kappa^2 d^2}f_{v2}, \\ S_m &= \begin{cases} S_{m,orig}, & S_{m,orig} \geq -c_{v2}\Omega \\ \dfrac{\Omega(c_{v2}^2\Omega + c_{v3}S_{m,orig})}{(c_{v3}-2.0c_{v2})\Omega - S_{m,orig}}, & \text{otherwise.}\end{cases} \end{aligned} \tag{20}$$

which, again, is consistent with Equation (5).

3 Comments

The complexity, and consequently length, of the source terms increase with both dimension and physics handled by the governing equations. Applying commands in order to simplify extensive expressions is challenging even with a high performance workstation; thus, a suitable alternative to this issue is to simplify each equation by dividing it into a combination of sub-operators handling different physical phenomena. Then, each one of the operators may be applied to the manufactured solutions individually, and the resulting sub-source terms are combined back to represent the source term for the original equation.

For instance, instead of writing the two-dimensional FANS SA equation using one single operator $\mathcal{L}$:

$$\mathcal{L} = \frac{\partial(\bar{\rho}\nu_{\text{sa}})}{\partial t} + \nabla\cdot(\bar{\rho}\tilde{\boldsymbol{u}}\nu_{\text{sa}}) - c_{b1}S_{\text{sa}}\bar{\rho}\nu_{\text{sa}} + c_{w1}f_w\bar{\rho}\left(\frac{\nu_{\text{sa}}}{d}\right)^2 - \frac{1}{\sigma}\nabla\cdot((\bar{\mu}+\bar{\rho}\nu_{\text{sa}})\nabla\nu_{\text{sa}}) - \frac{c_{b2}\bar{\rho}}{\sigma}\nabla\nu_{\text{sa}}\cdot\nabla\nu_{\text{sa}} \tag{21}$$

to then be used in the MMS, let Equation (21) be written with six operators:

$$\begin{aligned}
\mathcal{L}_1 &= \frac{\partial(\bar{\rho}\nu_{\text{sa}})}{\partial t}, & \mathcal{L}_2 &= \nabla\cdot(\bar{\rho}\tilde{\boldsymbol{u}}\nu_{\text{sa}}),\\
\mathcal{L}_3 &= -c_{b1}S_{\text{sa}}\bar{\rho}\nu_{\text{sa}}, & \mathcal{L}_4 &= c_{w1}f_w\bar{\rho}\left(\frac{\nu_{\text{sa}}}{d}\right)^2,\\
\mathcal{L}_5 &= -\frac{1}{\sigma}\nabla\cdot((\bar{\mu}+\bar{\rho}\nu_{\text{sa}})\nabla\nu_{\text{sa}}) & \mathcal{L}_6 &= -\frac{c_{b2}\bar{\rho}}{\sigma}\nabla\nu_{\text{sa}}\cdot\nabla\nu_{\text{sa}}.
\end{aligned} \tag{22}$$

Naturally, $\mathcal{L} = \mathcal{L}_1 + \mathcal{L}_2 + \mathcal{L}_3 + \mathcal{L}_4 + \mathcal{L}_5 + \mathcal{L}_6$.

After the application of each sub-operator defined in (22), the corresponding sub-source terms are also simplified, factorized and sorted. Then, the final factorized version is checked against the original one, in order to assure that not human error has been introduced.

An advantage of this strategy is the possibility of inclusion and/or removal of other physical effects without the need of re-doing previous manipulations. For instance, in order to simplify this model, assuming that the distance d to the nearest wall is infinite, changes should be made in only two operators: $\mathcal{L}_3$ is simplified since S_{sa} is reduced to $S_{\text{sa}} = \Omega$, and $\mathcal{L}_4 = 0$. The equations for conservation of mass, momentum and total energy remain unchanged.

This strategy results in less time, decreases the computational effort and occasional software crashes, and also increases the flexibility in the code verification procedure.

3.1 Boundary Conditions and C Files

Additionally to verifying code capability of solving the governing equations accurately in the interior of the domain of interest, one may also verify the software capability of correctly imposing boundary conditions. Therefore, the gradients of the analytical solutions (6) have been calculated:

$$\nabla\rho = \begin{bmatrix} \dfrac{1}{14}\dfrac{p_0}{RT^2}\dfrac{r_T(\gamma-1)M_\infty^2 T_\infty u_\tau}{u_\infty^2 x}u\cos\left(\dfrac{Au_{eq}}{u_\infty}\right)\left[y^+\frac{du_{eq}^+}{dy^+}+u_{eq}^+\right] \\ -\dfrac{p_0}{RT^2}\dfrac{r_T(\gamma-1)M_\infty^2 T_\infty u_\tau y^+}{u_\infty^2 y}u\cos\left(\dfrac{Au_{eq}}{u_\infty}\right)\frac{du_{eq}^+}{dy^+} \end{bmatrix},$$

$$\nabla T = \begin{bmatrix} -\dfrac{1}{14}\dfrac{r_T(\gamma-1)M_\infty^2 T_\infty u_\tau}{u_\infty^2 x}u\cos\left(\dfrac{Au_{eq}}{u_\infty}\right)\left[y^+\frac{du_{eq}^+}{dy^+}+u_{eq}^+\right] \\ \dfrac{r_T(\gamma-1)M_\infty^2 T_\infty u_\tau y^+}{u_\infty^2 y}u\cos\left(\dfrac{Au_{eq}}{u_\infty}\right)\frac{du_{eq}^+}{dy^+} \end{bmatrix},$$

$$\nabla u = \begin{bmatrix} -\dfrac{1}{14}\dfrac{u_\tau}{x}\cos\left(\dfrac{Au_{eq}}{u_\infty}\right)\left[y^+\frac{du_{eq}^+}{dy^+}+u_{eq}^+\right] \\ y^+\dfrac{u_\tau}{y}\frac{du_{eq}^+}{dy^+}\cos\left(\dfrac{Au_{eq}}{u_\infty}\right) \end{bmatrix}, \qquad \nabla v = \begin{bmatrix} -\dfrac{15}{196}\dfrac{\eta_v u_\tau y}{x^2} \\ \dfrac{1}{14}\dfrac{\eta_v u_\tau}{x} \end{bmatrix}$$

$$\nabla\nu_{\text{sa}} = \begin{bmatrix} -\dfrac{1}{14}\dfrac{\kappa u_\tau y}{x} \\ \kappa u_\tau - 2\alpha y \end{bmatrix}, \quad \text{and} \quad \nabla p = \begin{bmatrix} 0 \\ 0 \end{bmatrix}.$$

and translated into C codes:

```
grad_rho_an[0] = p_0 * T_inf * r_T * (double) (Gamma - 1) * M_inf * M_inf * sin(A * u_eq / u_inf)
  * cos(A * u_eq / u_inf) * u_tau * (u_eq_plus + y_plus * d_eqplus_yplus) / R
  * pow(T, -0.2e1) / A / u_inf / x / 0.14e2;
grad_rho_an[1] = -p_0 * T_inf * r_T * (double) (Gamma - 1) * M_inf * M_inf * sin(A * u_eq / u_inf)
  * cos(A * u_eq / u_inf) * y_plus * d_eqplus_yplus * u_tau / R * pow(T, -0.2e1) / A / u_inf / y;
grad_p_an[0] = 0;
grad_p_an[1] = 0;
grad_u_an[0] = -cos(A * u_eq / u_inf) * u_tau * (u_eq_plus + y_plus * d_eqplus_yplus) / x / 0.14e2;
grad_u_an[1] = cos(A * u_eq / u_inf) * y_plus * d_eqplus_yplus * u_tau / y;
grad_v_an[0] = -0.15e2 / 0.196e3 * eta_v * u_tau * y * pow(x, -0.2e1);
grad_v_an[1] = eta_v * u_tau / x / 0.14e2;
grad_T_an[0] = -T_inf * r_T * (double) (Gamma - 1) * M_inf * M_inf * sin(A * u_eq / u_inf)
  * cos(A * u_eq / u_inf) * u_tau * (u_eq_plus + y_plus * d_eqplus_yplus) / A / u_inf / x / 0.14e2;
grad_T_an[1] = T_inf * r_T * (double) (Gamma - 1) * M_inf * M_inf * sin(A * u_eq / u_inf)
  * cos(A * u_eq / u_inf) * y_plus * d_eqplus_yplus * u_tau / A / u_inf / y;
grad_nu_sa_an[0] = -kappa * u_tau * y / x / 0.14e2;
grad_nu_sa_an[1] = kappa * u_tau - 0.2e1 * alpha * y;
```

Files containing C codes for the source terms have also been automatically generated. They are: `FANS_SA_steady_2d_rho_code.C`, `FANS_SA_steady_2d_u_code.C`, `FANS_SA_steady_2d_v_code.C`, `FANS_SA_steady_2d_E_code.C` and `FANS_SA_steady_2d_nu_code.C`.

An example of the C file from the source term $Q_{\nu_{sa}}$ for the 2D Spalart–Allmaras equation is:

```
#include <math.h>

double SourceQ_nu (double x, double y)
{
  double Q_nu;
  double RHO;
  double U;
  double V;
  double T;
  double NU_SA;
  double Re_x;
  double c_f;
  double u_tau;
  double y_plus;
  double u_eq_plus;
  double u_eq;
  double d_eqplus_yplus;
  double mu_t;
  double chi;
  double f_v1;
  double f_v2;
  double Sm_orig;
  double Sm1;
  double Sm2;
  double Sm;
  double S_sa;
  double Omega;
  double f_w;
  double g;
  double r;
  Re_x = rho_inf * u_inf * x / mu;
  c_f = C_cf / F_c * pow(0.1e1 / F_c * Re_x, -0.1e1 / 0.7e1);
  u_tau = u_inf * sqrt(c_f / 0.2e1);
  y_plus = y * u_tau / nu_w;
  u_eq_plus = 0.1e1 / kappa * log(0.1e1 + kappa * y_plus)
    + C1 * (0.1e1 - exp(-y_plus / eta1) - y_plus / eta1 * exp(-y_plus * b));
  u_eq = u_tau * u_eq_plus;
  d_eqplus_yplus = 0.1e1 / (0.1e1 + kappa * y_plus)
    + C1 * (exp(-y_plus / eta1) / eta1 - exp(-y_plus * b) / eta1 + y_plus * b * exp(-y_plus * b) / eta1);
  U = u_inf / A * sin(A / u_inf * u_eq);
  V = eta_v * u_tau * y / x / 0.14e2;
  T = T_inf * (0.1e1 - r_T * (double) (Gamma - 1) * M_inf * M_inf * (0.1e1 - U * U * pow(u_inf, -0.2e1)) / 0.2e1);
  RHO = p_0 / R / T;
  NU_SA = kappa * u_tau * y - alpha * y * y;
```

```
  chi = RHO * NU_SA / mu;
  f_v1 = pow(chi, 0.3e1) / (pow(chi, 0.3e1) + pow(c_v1, 0.3e1));
  f_v2 = 0.1e1 - chi / (0.1e1 + chi * f_v1);
  Omega = sqrt(pow(0.196e3 * x * x * y_plus * d_eqplus_yplus * cos(A / u_inf * u_eq) + 0.15e2 * eta_v * y * y, 0.2e1)
    * u_tau * u_tau * pow(x, -0.4e1) * pow(y, -0.2e1)) / 0.196e3;
  Sm_orig = NU_SA * pow(kappa, -0.2e1) * pow(d, -0.2e1) * f_v2;
  Sm1 = Sm_orig;
  Sm2 = Omega * (c_v2 * c_v2 * Omega + c_v3 * Sm_orig) / ((cv_3 + (-0.1e1) * 0.20e1 * c_v2) * Omega - Sm_orig);
  if (-c_v2 * Omega <= Sm_orig)
    Sm = Sm1;
  else
    Sm = Sm2;
  S_sa = Sm + Omega;
  r = NU_SA / S_sa * pow(kappa, -0.2e1) * pow(d, -0.2e1);
  g = r + c_w2 * (pow(r, 0.6e1) - r);
  f_w = g * pow((0.1e1 + pow(c_w3, 0.6e1)) / (pow(g, 0.6e1) + pow(c_w3, 0.6e1)), 0.1e1 / 0.6e1);
  Q_nu = -r_T * (double) (Gamma - 1) * M_inf * M_inf * T_inf * y_plus * u_tau * d_eqplus_yplus * NU_SA * RHO * U * V
      * cos(A / u_inf * u_eq) * pow(u_inf, -0.2e1) / y / T
    + (double) (Gamma - 1) * (y_plus * d_eqplus_yplus + u_eq_plus) * y * kappa * r_T * M_inf * M_inf * T_inf * u_tau
      * u_tau * NU_SA * RHO * U * cos(A / u_inf * u_eq) / sigma * pow(u_inf, -0.2e1) * pow(x, -0.2e1) / T / 0.196e3
    - (double) (Gamma - 1) * (0.2e1 * alpha * y - kappa * u_tau) * r_T * M_inf * M_inf * T_inf * y_plus * u_tau
      * d_eqplus_yplus * NU_SA * RHO * U * cos(A / u_inf * u_eq) / sigma * pow(u_inf, -0.2e1) / y / T
    + (double) (Gamma - 1) * (y_plus * d_eqplus_yplus + u_eq_plus) * r_T * M_inf * M_inf * T_inf * u_tau
      * NU_SA * RHO * U * U * cos(A / u_inf * u_eq) * pow(u_inf, -0.2e1) / x / T / 0.14e2
    - (double) (1 + c_b2) * y * y * kappa * kappa * u_tau * u_tau * RHO / sigma * pow(x, -0.2e1) / 0.196e3
    - kappa * u_tau * y * RHO * U / x / 0.14e2
    - (y_plus * d_eqplus_yplus + u_eq_plus) * u_tau * NU_SA * RHO * cos(A / u_inf * u_eq) / x / 0.14e2
    + c_w1 * f_w * NU_SA * NU_SA * RHO * pow(d, -0.2e1)
    + RHO * NU_SA * V / y
    - S_sa * c_b1 * NU_SA * RHO
    + (-0.2e1 * alpha * y + kappa * u_tau) * RHO * V
    - pow(0.2e1 * alpha * y - kappa * u_tau, 0.2e1) * (double) (1 + c_b2) * RHO / sigma
    + (RHO * NU_SA + mu) * (0.392e3 * alpha * x * x - 0.15e2 * kappa * u_tau * y) / sigma * pow(x, -0.2e1) / 0.196e3;
  return(Q_nu);
}
```

References

Cebeci, T., K. Chang, and P. Bradshaw (1980). Solution Of A Hyperbolic System Of Turbulence-Model Equations By The Box Scheme. *Computer Methods In Applied Mechanics And Engineering 22*(2), 213–227.

Chi, S. and D. Spalding (1966). Influence Of Temperature Ratio On Heat Transfer To A Flat Plate Through A Turbulent Boundary Layer In Air. *Chemical Engineering Progress 62*(7), 80–&.

Eça, L., M. Hoekstra, A. Hay, and D. Pelletier (2007, DEC). Verification of RANS solvers with manufactured solutions. *Engineering With Computers 23*(4), 253–270.

Maplesoft (2010, November). Maple: the essential tool for mathematics and modeling. http://www.maplesoft.com/Products/Maple/.

Oliver, T. A. (2010). Favre-Averaged Navier-Stokes and Turbulence Model Equation Documentation. Technical report, Intitute for Computational Engineering and Sciences of the University of Texas, Austin.

Spalart, P. R. and S. A. Allmaras (1994). A one-equation turbulence model for aerodynamic flows. *La Recherche Aerospatiale 1*, 5–21. See also AIAA Paper 1992-439.

Van Driest, E. R. (1956, October). Problem of aerodynamic heating. *Aeron. Eng. Rev. 15*(10), 26–41.

White, F. M. (1991). *Viscous Fluid Flow* (Second Edition ed.). McGraw-Hill.

A A Physically-based Manufactured Solution for FANS–SA Equations

To exercise all of the terms in the equation, the solution must satisfy the no slip wall boundary condition for at least some portion of the boundary. To avoid pathological behavior in the solution and required source terms, we strive to make the manufactured solution reasonably resemble the inner portion (viscous sublayer + logarithmic layer) of a zero pressure gradient boundary layer. To accomplish this goal, the manufactured solution is built using well-known correlations for turbulent boundary layers. The manufactured solution is developed in Sections A.1 through A.3. Some of the derivatives required to compute the manufactured source terms are given in Section A.4. The behavior of the solution is shown graphically for particular values of the constant parameters in Section C. To check the behavior of the SA model terms, the SA model budget is computed and shown in Section D.

A.1 Velocity Field

A.1.1 Streamwise Velocity

For the streamwise velocity, we construct the solution by working backward from the van Driest transformation. Inverting the adiabatic wall form of the van Driest transformation Van Driest (1956); White (1991) gives

$$u = \frac{u_\infty}{A} \sin\left(\frac{A}{u_\infty} u_{eq}\right), \tag{23}$$

where u_∞, $A = \sqrt{1 - T_\infty/T_{aw}}$, T_∞, and T_{aw} are constants, and u_{eq} is the van Driest equivalent velocity. The van Driest equivalent velocity can be computed from the friction velocity u_τ and the non-dimensionalized van Driest velocity $u_{eq}^+ \equiv u_{eq}/u_\tau$. Clearly,

$$u_{eq} = u_\tau u_{eq}^+. \tag{24}$$

Thus, to specify the velocity, one must specify u_τ and u_{eq}^+. The friction velocity can be determined from the skin friction coefficient:

$$u_\tau \equiv \sqrt{\frac{\tau_w}{\rho_w}} = u_\infty \sqrt{\frac{c_f}{2}}. \tag{25}$$

We model the skin friction coefficient using the compressibility transformation idea of Spalding and Chi Chi and Spalding (1966) and a correlation for the incompressible skin friction. Specifically,

$$c_f = \frac{1}{F_c} c_{f,inc}\left(\frac{1}{F_c} Re_x\right), \tag{26}$$

where

$$F_c = \frac{T_{aw}/T_\infty - 1}{\left(\sin^{-1} A\right)^2} \tag{27}$$

is a constant and $c_{f,inc}$ is a correlation for the incompressible skin friction. Specifically, we choose a power law for the incompressible skin friction coefficient:

$$c_{f,inc}(Re_x) = C_{cf} Re_x^{-1/7}, \tag{28}$$

where C_{cf} is a constant.

Finally, to complete the manufactured solution, we set u_{eq}^+ using the velocity profile model of Cebeci and Bradshaw Cebeci et al. (1980):

$$u_{eq}^+ = \frac{1}{\kappa} \log\left(1 + \kappa y^+\right) + C_1 \left[1 - e^{-y^+/\eta_1} - \frac{y^+}{\eta_1} e^{-y^+ b}\right], \tag{29}$$

where κ, η_1 and b are constants, and

$$C_1 = -(1/\kappa)\log(\kappa) + C. \tag{30}$$

$$y^+ \equiv \frac{y}{\ell_v}, \tag{31}$$

and

$$\ell_v \equiv \frac{\nu_w}{u_\tau}. \tag{32}$$

A.1.2 Wall-normal Velocity

Based on a crude order of magnitude analysis of the continuity equation, the wall-normal velocity component is set to:

$$v = -\eta_v \frac{du_\tau}{dx} y, \tag{33}$$

where η_v is a user-specified parameter.

A.2 Thermodynamic State

For the mean temperature, we write:

$$T = T_\infty \left[1 + r_T \frac{\gamma - 1}{2} M_\infty^2 \left(1 - \left(\frac{u}{u_e} \right)^2 \right) \right], \tag{34}$$

where T_∞, r, and γ are additional constant parameters. Note that the constant T_{aw} is defined as $T_{aw} = T(u = 0)$.

Choosing the pressure to be a constant $p = p_0$, the density can be computed from the ideal gas equation:

$$\rho = \frac{p_0}{RT}, \tag{35}$$

where R is the gas constant.

A.3 Spalart-Allmaras Variable

The velocity profile manufactured solution constructed above is intended to be a reasonable representation of the viscous sublayer and log layer in a zero pressure gradient boundary layer. In this region in an incompressible boundary layer, the SA model is designed to give $\nu_{\mathrm{sa}}/\nu = \kappa y^+$. Based on this form, we choose

$$\nu_{\mathrm{sa}} = \kappa u_\tau y - \alpha y^2, \tag{36}$$

where α is a constant. The y^2 term is included simply to make the solution nonlinear in y.

A.4 Manufactured Solution's Spatial Derivatives

In the Equation (23) for the streamwise velocity, the values u_∞ and A are constants. Thus,

$$\frac{\partial u}{\partial x} = \cos\left(\frac{A}{u_\infty} u_{eq} \right) \frac{\partial u_{eq}}{\partial x}, \quad \text{and} \quad \frac{\partial u}{\partial y} = \cos\left(\frac{A}{u_\infty} u_{eq} \right) \frac{\partial u_{eq}}{\partial y}.$$

The parameter u_τ in the van Driest equivalent velocity equation (24) is a function of x only, and u_{eq}^+ is a function of $y^+ \equiv (y u_\tau)/\nu_w$. Thus,

$$\frac{\partial u_{eq}}{\partial x} = \frac{du_\tau}{dx} u_{eq}^+ + u_\tau \frac{du_{eq}^+}{dy^+} \frac{\partial y^+}{\partial x} \quad \text{and} \quad \frac{\partial u_{eq}}{\partial y} = u_\tau \frac{du_{eq}^+}{dy^+} \frac{\partial y^+}{\partial y},$$

where

$$\frac{\partial y^+}{\partial x} = \frac{y}{\nu_w} \frac{du_\tau}{dx}, \quad \text{and} \quad \frac{\partial y^+}{\partial y} = \frac{u_\tau}{\nu_w}.$$

The derivative of the friction velocity (25) is given by

$$\frac{du_\tau}{dx} = u_\infty \frac{1}{2} \sqrt{\frac{2}{c_f}} \frac{dc_f}{dx}.$$

where

$$\frac{dc_f}{dx} = -\frac{C_{cf}}{F_c} \frac{1}{7} \left(\frac{1}{F_c} Re_x \right)^{-8/7} \frac{1}{F_c} \frac{\rho_\infty u_\infty}{\mu}$$

since C_{cf}, F_c, ρ_∞, u_∞, and μ are constants in Equations (27) and (28).

Finally, the derivative of the non-dimensionalized van Driest velocity profile (29) is given by

$$\frac{du_{eq}^+}{dy^+} = \frac{1}{(1+\kappa y^+)} + C_1\left[\frac{1}{\eta_1}e^{-y^+/\eta_1} - \frac{1}{\eta_1}e^{-y^+b} + b\frac{y^+}{\eta_1}e^{-y^+b}\right].$$

The derivatives of the wall-normal velocity equation (33) with respect to x and y are simply:

$$\frac{\partial v}{\partial x} = -\eta_v \frac{d^2u_\tau}{dx^2}y, \quad \text{and} \quad \frac{\partial v}{\partial y} = -\eta_v \frac{du_\tau}{dx}.$$

Temperature and density are given by Equations (34) and (35). Their derivatives are, respectively:

$$\frac{\partial T}{\partial x} = T_\infty\left[r_T\frac{\gamma-1}{2}M_\infty^2\left(-2\left(\frac{u}{u_\infty}\right)\frac{1}{u_\infty}\frac{\partial u}{\partial x}\right)\right], \quad \text{and} \quad \frac{\partial T}{\partial y} = T_\infty\left[r_T\frac{\gamma-1}{2}M_\infty^2\left(-2\left(\frac{u}{u_\infty}\right)\frac{1}{u_\infty}\frac{\partial u}{\partial y}\right)\right],$$

and

$$\frac{\partial \rho}{\partial x} = -\frac{p_0}{RT^2}\frac{\partial T}{\partial x}, \quad \text{and} \quad \frac{\partial \rho}{\partial y} = -\frac{p_0}{RT^2}\frac{\partial T}{\partial y}.$$

Finally, the derivatives of the SA state variable (36) are given by:

$$\frac{\partial \nu_{\mathrm{sa}}}{\partial x} = \kappa\frac{du_\tau}{dx}y, \quad \text{and} \quad \frac{\partial \nu_{\mathrm{sa}}}{\partial y} = \kappa u_\tau - 2\alpha y.$$

B Parameters and Constants

This section summarizes the parameters of the manufactured solution and source terms. For completeness, a list of constants that can be computed from the parameters is also given. Table 1 details the parameters of the manufactured solution. In addition to the solution parameters, there are a number of parameters required to specify the source term required by the method of manufactured solutions. Table 2 details these parameters. There are a number of additional constants that appear in the solution and that can be computed from the parameters. These constants should not be user-specified parameters. They are listed in Table 3.

Table 1: Parameters required to specify manufactured solution.

Parameter	Nom. Val.	Units	Eqn(s)	Explanation
C_{cf}	0.027	NA	28	Incompressible skin friction fit parameter.
κ	0.41	NA	29, 36, 30	von Karman constant (incompressible profile and SA).
η_1	11.0	NA	29	Incompressible velocity profile model.
b	0.33	NA	29	Incompressible velocity profile model.
C	5.0	NA	30	Incompressible velocity profile model.
η_v	30.0	NA	33	Wall normal velocity parameter.
T_∞	250.0	K	34	Freestream temperature.
M_∞	0.8	NA	34	Freestream Mach number.
r	0.9	NA	34	Recovery factor.
γ	1.4	NA	34	Ratio of specific heats = c_p/c_v.
p_0	1e4	N/m^2	35	Mean pressure (constant throughout domain).
R	287.0	J/(kg K)	35	Gas constant = $c_p - c_v$.
α	5.0	1/s	36	Eddy viscosity quadratic term parameter.

Table 2: Additional parameters required to specify source terms.

Parameter	Nom. Val.	Units	Explanation
μ	1e-4	kg/(m s)	Fluid dynamic viscosity (constant throughout domain).
Pr	0.71	NA	Prandtl number.
Pr_t	0.9	NA	Turbulent Prandtl number.
c_{b1}	0.1355	NA	SA model parameter.
σ_{sa}	2.0/3.0	NA	SA model parameter.
c_{b2}	0.622	NA	SA model parameter.
c_{w2}	0.3	NA	SA model parameter.
c_{w3}	2.0	NA	SA model parameter.
c_{v1}	7.1	NA	SA model parameter.
c_{v2}	??	NA	SA model parameter.
c_{v3}	??	NA	SA model parameter.

Table 3: Additional constants that can be computed from the parameters.

Constant	Expression	Eqn(s)	Explanation
u_∞	$M_\infty\sqrt{\gamma R T_\infty}$	23, 25	Freestream velocity.
ρ_w	$p_0/(RT_{aw})$	25	Density at the wall.
F_c	$(T_{aw}/T_\infty - 1)/(\sin^{-1} A)^2$	27, 26	Skin friction transformation parameter.
T_{aw}	$T_\infty\left[1 + r\frac{\gamma-1}{2}M_\infty^2\right]$	34	Wall temperature.
ρ_∞	$p_0/(RT_\infty)$	Used to compute Re_x	Freestream density.
ν_w	μ/ρ_w	32	Kinematic viscosity at the wall.
A	$\sqrt{1 - T_\infty/T_{aw}}$	23, 27	Constant in van Driest transform.
c_p	$(\gamma R)/(\gamma - 1)$		Specific heat at constant pressure.
c_v	$R/(\gamma - 1)$		Specific heat at constant volume.
c_{w1}	$c_{b1}/\kappa^2 + (1 + c_{b2})/\sigma_{\text{sa}}$		SA equation constant.

C Solution Plots

This section shows the manufactured solution as a function of y at $x = 0.75$ m for particular choices of the values of the constant parameters. The figures was generated using the following values of the non-dimensional parameters:

$$
\begin{aligned}
\kappa &= 0.41, & C &= 5.00, & \eta_1 &= 11,\\
b &= 0.33, & r &= 0.9, & \gamma &= 1.4,\\
M_\infty &= 0.8, & C_{cf} &= 0.027, & \eta_v &= 30,\\
c_{b1} &= 0.1355, & \sigma_{SA} &= \tfrac{2}{3}, & c_{b2} &= 0.622,\\
c_{w2} &= 0.3, & c_{w3} &= 2, & c_{v1} &= 7.1.
\end{aligned}
$$

The dimensional parameters are as follows:

$$
\begin{aligned}
T_\infty &= 250\,\text{K}, & p_0 &= 1\times 10^4\,\text{N/m}^2, \quad R = 287.0\,\text{J/(kgK)},\\
\mu &= 1\times 10^{-4}\,\text{kg/(ms)}, & \alpha &= 5\,\text{m}^2/\text{s}.
\end{aligned}
$$

These parameter values give reasonable behavior of the manufactured solution and source terms and are the recommended values. Figure 1(a) shows the u and v velocity profiles, Figure 1(b) shows the ρ and T profiles, and Figure 1(c) shows the ν_{sa} and χ profiles.

D SA Equation Budget

The stated goal of this work is to develop a manufactured solution that reasonably resembles a boundary layer. This is most crucial with respect to the turbulence model. As demonstrated by Eça et al. (2007), the observed

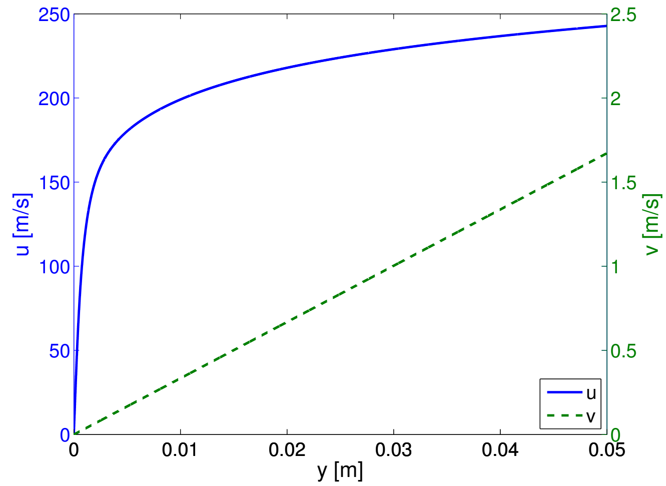

(a) The manufactured velocity profiles.

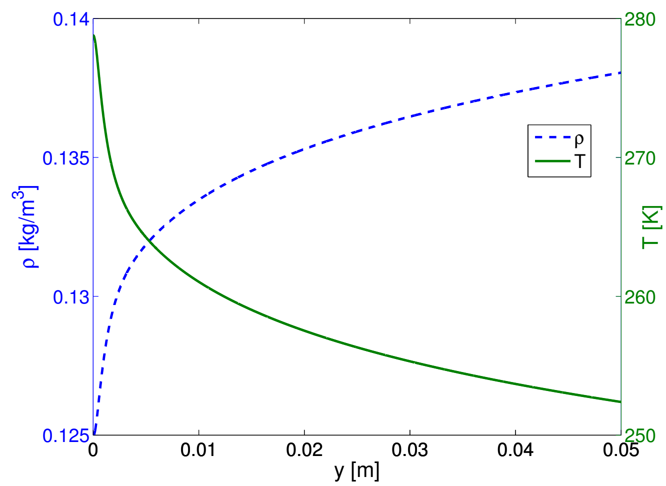

(b) The manufactured density and temperature profiles.

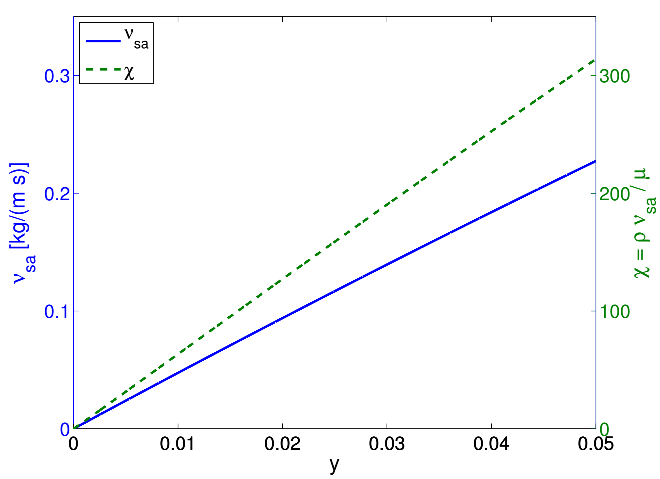

(c) The manufactured ν_{sa} and χ profiles.

Figure 1: Manufactured solutions profiles.

behavior of the turbulence model can be highly sensitive to the chosen manufactured solution. To evaluate the current choices, we plot the SA model equation budget. The figures was generated using the parameter values given in Section C. The curve labeled "Sum" is equal to the sum of all of the SA terms collected on the left hand side—i.e., it is the residual of the SA equation evaluated at the manufactured state. This residual is equivalent to the source term that must be added to the right hand side to balance the equation such that the manufactured state is a solution.

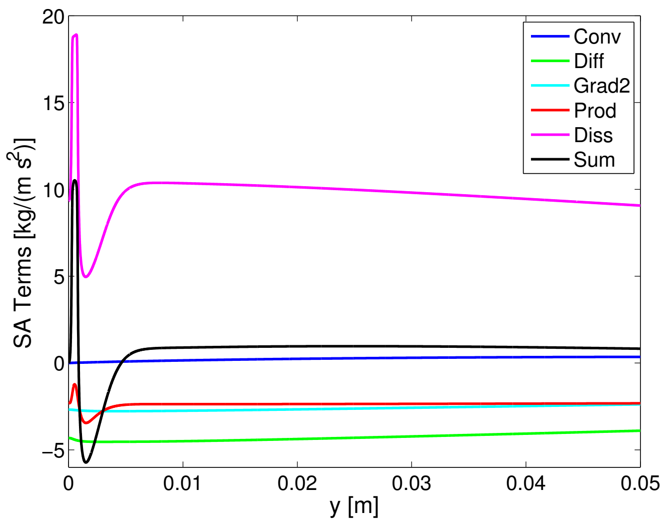

Figure 2: The Spalart-Allmaras model equation budget.

Figure 2 shows that for $y > 0.006\,\mathrm{m} \approx 100\ell_v$ the expected log layer behavior is roughly achieved. All of the SA terms except convection are significant and nearly in balance (i.e., the residual term is significantly smaller than any of the individual terms except convection). For $y < 0.006\,\mathrm{m}$, the is residual is more significant, mostly due to the dissipation term.

Figure 3 shows the budget in this region more clearly. Very close to the wall ($0 \le y \le 1 \times 10^{-4} \approx 2\ell_v$) the terms have the behavior expected in the viscous sublayer, and the residual is small. It appears that the large residual region is associated with the transition from viscous sublayer behavior to log layer behavior. There is no reason to expect that the manufactured solution constructed in this work is close to the true SA model solution in this region. Thus, it is reasonable for the SA equation to be more out of balance, leading to the larger residual in this region.

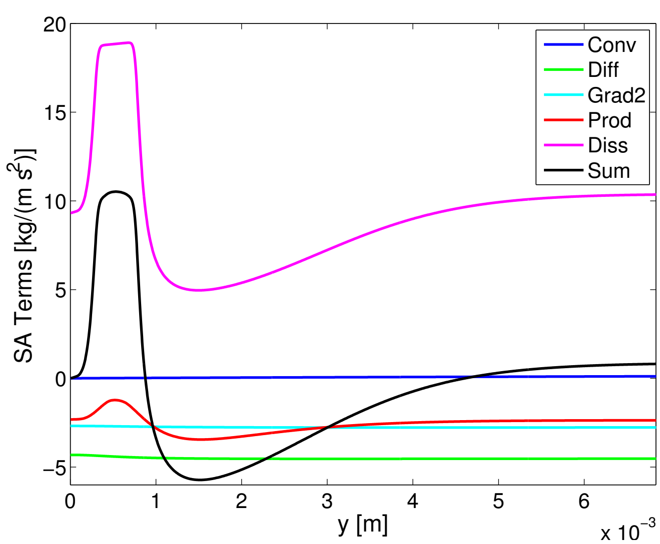

Figure 3: The Spalart-Allmaras model equation budget very close to the wall ($0 \le y \le 100\ell_v$).